buildings

MDPI

Article

Experimental Study on the Preparation and Properties of Alkali-Activated Slag-Based Flow Solidified Soil

Haitao Ma [1], Guangbiao Shao [2,*], Dexiang Hou [1], Wanpeng Li [2], Daoyuan Zhao [1] and Jianyong Han [2]

[1] Jinan Luyuan Electric Group Co., Ltd., Jinan 250000, China; linfeng8842@163.com (H.M.); 13793145653@163.com (D.H.); zdy9706@163.com (D.Z.)
[2] School of Civil Engineering, Shandong Jianzhu University, Jinan 250101, China; 18563050907@163.com (W.L.); hanlwb@163.com (J.H.)
* Correspondence: shaogb@sdjzu.edu.cn

Abstract

To promote the resource recovery and utilization of construction spoil and to prepare flowable solidified soil with tunable properties and excellent construction adaptability, locally sourced construction spoil from Jinan was used as the primary raw material. A slag-based solidifying agent composed of cement, slag, fly ash, and desulfurized gypsum was prepared, together with a composite alkaline activation system consisting of calcium hydroxide and anhydrous sodium sulfate. The effects of solidifying-agent content, alkaline activator dosage, and slag-to-fly ash proportion on the workability, mechanical properties, and permeability of the flowable solidified soil were systematically investigated. The results show that solidifying-agent content significantly affects the material properties. As the content increased from 10% to 30%, the 28-day compressive strength increased from 0.94 MPa to 5.43 MPa, while the permeability coefficient decreased substantially; the best flowability occurred at intermediate contents. As the alkaline activator dosage increased from 1.8% to 4.8%, the slurry flow spread decreased from 214 mm to 193 mm and the bleeding rate decreased from 2.4% to 0.3%, while the 28-day compressive strength increased from 0.68 MPa to 0.92 MPa, indicating that alkaline activation markedly improves the water-retention capacity and mechanical properties of the solidified system. The slag-to-fly ash proportion regulates material performance through the synergistic effects of physical filling and chemical reactivity. Increasing the fly ash content improves slurry flowability but adversely affects strength development. These results provide experimental evidence and a theoretical basis for mix-proportion optimization and subsequent engineering application of alkali-activated slag-based flowable solidified soil.

Keywords: flowable solidified soil; construction spoil; solidifying agent; flow spread; unconfined compressive strength; bleeding rate

Check for updates

Academic Editor: Ahmed Senouci

Received: 20 July 2026
Revised: 6 September 2026
Accepted: 8 September 2026
Published: 17 September 2026

Copyright: © 2026 by the authors. Licensee MDPI, Basel, Switzerland. This article is an open access article distributed under the terms and conditions of the Creative Commons Attribution (CC BY) license.

1. Introduction

In recent years, with the acceleration of urbanization, the resource utilization of construction spoil and construction waste has become a research focus in geotechnical engineering and materials science. Flowable solidified soil is a green construction material in which solidifying agents are incorporated to improve the engineering properties of soil. Owing to its good flowability, self-compaction, controllable strength, and environmental benefits, it has broad application potential in trench backfilling, subgrade engineering, and sludge solidification. Current research mainly focuses on optimizing solidifying-agent

proportions, enhancing mechanical properties, and improving durability, and numerous laboratory studies and field applications have advanced both the theoretical development and engineering implementation of this technology. Thus, while enabling the beneficial utilization of various engineering wastes, flowable solidified soil is also cost-effective and has broad prospects for backfilling and ground-improvement applications requiring relatively low strength.

Regarding the type and proportioning of solidifying agents, numerous studies have clarified the mechanisms of inorganic and composite binders. Lai et al. [1] systematically investigated mixture proportions and demonstrated the significant effects of cement content (5–10%) and water-to-solid ratio (0.35–0.50) on unconfined compressive strength (UCS); when the binder-to-soil ratio increased to 10%, the UCS increased by approximately three-fold, whereas an excessive water-to-solid ratio caused strength deterioration. Dai et al. [2] compared cement-blast-furnace slag, cement-phosphogypsum, and cement-fly ash composite systems and reported that the cement-blast-furnace slag system at a mass ratio of 50:50 provided the best overall performance, with a flow spread of 255 mm and a 28-day strength of 0.97 MPa. Li et al. [3] further investigated the effects of single and combined additions of hydrated lime, cement, and fly ash on flowability and identified a water-to-solid ratio of 0.20 as a critical value for flowability; a water-reducer dosage of 1.5% satisfied pumping requirements. Zhou et al. [4] described premixed solidified soil from a materials perspective and emphasized that a combination of composite mineral design and chemical activation can fill pores among soil particles and densify the structure. Su et al. [5] reviewed the pozzolanic effects of industrial solid wastes such as slag and fly ash and found that blended systems can activate secondary hydration reactions, generating C-S-H gel and ettringite and thereby improving long-term strength. Zhu et al. [6], through a project case in the Maozhou River area of Dongguan, verified the effectiveness of a sulfoaluminate-cement-based solidifying agent for early-strength flowable backfill; at a binder-to-sand ratio of 0.15 and a water-to-solid ratio of 0.63, the strength at 2 h reached 24 kPa. Lyu et al. [7] showed from the perspective of curing regimes that early-age curing conditions can significantly alter strength development and microstructural evolution, and that macroscopic performance is closely related to internal reaction processes under different curing conditions. These studies indicate that the final engineering performance of cementitious materials depends not only on raw-material composition but also on hydration, pore-structure evolution, and curing conditions. Recent studies have also demonstrated the feasibility of converting excavated waste muck into value-added construction materials. Sun et al. [8] utilized shield waste muck to prepare modified synchronous grouting materials and optimized the mixture proportions while further evaluating their environmental and economic benefits.

With respect to physical and mechanical properties, research has focused on the relationships among strength, flowability, bleeding rate, and permeability. Wang et al. [9] investigated the impermeability and its formation mechanism in alkali-activated slag-based flowable solidified soil. Their results showed that increasing solidifying-agent content promoted the formation of abundant C-S-H gel and ettringite that filled soil pores and densified the structure, reducing the 28-day permeability coefficient to 10^{-8} cm/s and satisfying low-permeability requirements for pollution-control applications. Xie et al. [10] studied the effects of polycarboxylate superplasticizer, phosphogypsum, and sodium silicate on the permeability of flowable solidified soil prepared from pipe-jacking spoil. The synergistic action of phosphogypsum and sodium silicate promoted the formation of ettringite and C-S-H gel, filled soil pores, and significantly increased structural compactness, reducing the 28-day permeability coefficient to 1.2×10^{-8}–3.7×10^{-8} cm/s. Chi et al. [11] investigated a multi-component slag-cement composite solidifying agent for flowable solidified soil in Shanghai and found that increasing solidifying-agent content generated abundant C-A-S-H

gel and ettringite, forming a dense skeleton; the maximum 28-day UCS reached 1.74 MPa, approximately 172% higher than that at the lower dosage, significantly improving the bearing capacity of high-clay-content soft soil. Hao et al. [12] investigated cement blended with an all-solid-waste low-carbon cementitious material and found that the best performance for silt was obtained with 80% all-solid-waste cementitious material and 20% cement. At a water-to-solid ratio of 0.4, the 28-day UCS was approximately 3.35 times that of the pure solid-waste system and approximately 1.26 times that of the pure-cement system, indicating improved mechanical capacity and early-strength development. In addition to stabilizer type and mix proportion, microstructural evolution of the cementitious system is also an important factor governing macroscopic engineering performance. Previous studies have shown that regulating hydration reactions and pore structure in cement-based materials can further improve mechanical performance and durability. Feng et al. [13] investigated the effects of nanomaterials of different dimensionalities on cement paste and found that various nanomaterials can promote early hydration, refine pore structure, and reduce overall porosity to different extents, thereby improving early-age mechanical performance. These findings suggest a potential competition between workability and mechanical performance in cementitious systems.

Current materials used for soil stabilization and improvement mainly include conventional Ca-based stabilizers, ionic stabilizers, polymer/polyelectrolyte stabilizers, and cement-mineral-admixture composite cementitious systems. Ca-based stabilizers can effectively improve soil strength and shrink–swell behavior, but their efficiency depends on the mineralogical composition of the parent soil and environmental conditions. Ionic stabilizers primarily improve particle aggregation and shrink–swell characteristics by modifying the electrochemical environment at clay-particle surfaces, but may provide limited strength enhancement when used alone. Polymer and polyelectrolyte stabilizers are generally effective at low dosages; however, their long-term durability, cost-effectiveness, and applicability to different soil types require further evaluation. In comparison, composite cementitious systems composed of cement, slag, fly ash, and related mineral admixtures provide greater flexibility for balancing workability, mechanical properties, and permeability by adjusting constituent proportions.The characteristics of various soil solidifying agents are summarized in Table 1.

Existing soil-stabilization technologies differ in their primary performance benefits. Conventional Ca-based and ionic stabilizers mainly target soil strength, shrink–swell behavior, and volumetric stability, whereas polymers and polyelectrolytes can improve interparticle bonding and mechanical properties at relatively low dosages. By contrast, composite mineral cementitious systems based on cement, slag, and fly ash provide a broader compositional design space, allowing different performance indices to be tailored to specific engineering requirements.

However, the engineering performance of flowable solidified soil does not improve uniformly with increasing content of any single constituent; trade-offs commonly exist among different performance indicators. For example, increasing the binder or slag proportion is generally beneficial to strength development but may reduce slurry flowability, whereas increasing the fly ash proportion can improve flowability but may adversely affect strength development. Therefore, evaluating a mix proportion solely on the basis of strength cannot adequately characterize the overall engineering performance of flowable solidified soil.

Table 1. Comparison of representative soil stabilization systems and their engineering characteristics.

Stabilization System	Representative Materials	Representative Dosage Reported in the Literature	Main Improvement Effects	Main Advantages	Main Limitations	Applicable Soils/Engineering Scenarios
Ca-based stabilizers	Sugarcane bagasse ash (SCBA), waste marble dust (WMD), and other Ca-rich materials	SCBA ≈ 4%; WMD ≈ 10%	Reduces plasticity index, swell, and swelling pressure, and improves strength [14]	Readily available; effective control of swelling; enables industrial/agricultural waste utilization	Effect depends on soil mineralogy, Ca content, and curing conditions	Expansive soils, subgrades, and shallow ground improvement
Liquid ionic stabilizer	Liquid ionic soil stabilizer (LISS)	Solution treatment ratios of 1:300 and 1:150	Markedly reduces swelling deformation and increases stiffness, but provides limited UCS improvement [15]	Low dosage; suitable for in situ treatment; markedly improves volumetric stability	Strength gain may be limited; effectiveness depends on clay mineralogy and ionic environment	Highly expansive clays and in situ ground treatment
Polymer/polyelectrolyte stabilizers	PSS, PDADMAC	0.2–3.2% of dry-soil mass	Improves UCS, toughness, and interparticle bonding; PSS increases 7 d UCS from about 1.5 MPa to 2.0–3.1 MPa [16]	Low dosage; enables targeted regulation of particle-surface interactions	Performance varies among polymers; long-term durability, environmental effects, and cost require evaluation	Improvement of expansive/special clays; currently mainly experimental
Fly ash–GGBS composite stabilizer	Fly ash + GGBS + a small amount of lime	FA:GGBS = 70:30; composite ≈ 20%, plus 1% lime	Reduces liquid limit, plasticity index, and swelling; increases UCS [17]	Synergistically utilizes low-Ca fly ash and high-Ca slag, reducing conventional binder use	Sensitive to mix proportion and activation conditions; reactivity may be insufficient when used alone	Expansive soils, subgrades, and ground improvement
Alkali-activated FA-GBFS geopolymer	Fly ash + blast-furnace slag + NaOH	FA 12–24%; GBFS 8–14%; NaOH 6–12 M	Increases UCS and CBR and reduces permeability	Wide compositional adjustability; can balance strength and impermeability; low-carbon potential	Complex mix design; activator concentration and FA/GBFS ratio affect performance	High-plasticity clays, ground stabilization, and subgrades
Composite system in this study	Cement + slag + fly ash + desulfurized gypsum + $Ca(OH)_2$/Na_2SO_4	Solidifying agent 10–30%; alkaline activator 1.8–4.8%; slag/fly ash 1:1–1:2	Regulates flow spread, bleeding rate, UCS, and permeability coefficient [18]	Targets beneficial use of excavated soil; evaluates workability, mechanical performance, and impermeability concurrently	Currently based on single-factor tests; multifactor interactions not quantified; lacks direct microstructural characterization	Flowable backfill using excavated soil, trench backfill, and related low-strength filling

Based on these considerations, this study uses excavated engineering soil from Jinan as the primary raw material and develops a composite solidifying system consisting of cement, slag, fly ash, and desulfurized gypsum, together with a $Ca(OH)_2$–Na_2SO_4 composite alkaline activation system, with the aim of promoting the resource utilization of slag, fly ash, and other industrial solid wastes in flowable solidified soil. The main contribution of this study does not lie in the single-factor experimental method itself, but rather in the application of an alkali-activated slag–fly ash composite cementitious system to the preparation of flowable solidified soil using excavated engineering soil. Under a consistent raw-material framework, the effects of solidifying-agent content, alkaline activator dosage, and slag-to-fly ash ratio on flow spread, bleeding rate, unconfined compressive strength, and permeability were systematically investigated. On this basis, the relationships and trade-offs among construction workability, mechanical performance, and impermeability were further analyzed to identify reasonable parameter ranges for this material system. The results are expected to provide an experimental basis for the mix design and engineering application of flowable backfill materials and similar controlled low-strength materials prepared from excavated engineering soil.

2. Materials and Methods

2.1. Experimental Materials

The soil used in the tests was construction spoil collected from a construction site in Jinan and consisted mainly of silty clay and silty sand. Its main chemical composition is listed in Table 2. Conventional geotechnical tests were conducted on the collected soil in accordance with the Standard for Geotechnical Testing Method (GB/T 50123-2019 [19]). The basic physical properties of the excavated soil are presented in Table 3. Particle-size analysis was conducted in accordance with the relevant test standard, and the particle-size distribution curve is shown in Figure 1. The characteristic particle sizes were obtained from the particle-size distribution curve, based on which the coefficient of uniformity (C_u) and coefficient of curvature (C_c) were determined. The engineering classification of the excavated soil was performed according to the relevant soil classification standard, considering both the particle-size distribution and consistency-limit indices.

Table 2. Main chemical composition of the construction spoil.

Chemical Composition	CaO	Al_2O_3	Fe_2O_3	SiO_2	MgO	K_2O	Na_2O	Others
Mass fraction/%	5.8	17.3	7.9	55.2	2.6	3.4	2.1	5.7

Table 3. Physical properties of the construction spoil.

Water Content/%	Liquid Limit/%	Plastic Limit/%	Plasticity Index	Coefficient of Curvature, C_c	Coefficient of Uniformity, C_u
17.5%	38.2%	21.7%	16.5	1.0	7.7

The solidifying agent used in the tests was a slag-based solidifying agent composed of cement, slag, fly ash, and desulfurized gypsum. The cement was 42.5-grade ordinary Portland cement, and the fly ash was Class F Grade I fly ash. As shown in Figure 2, the XRD pattern of the slag exhibits a broad diffuse halo at approximately $2\theta = 20°$~$35°$, indicating the presence of a substantial amorphous glassy phase. Several relatively sharp diffraction peaks are superimposed on this broad background, suggesting that the slag is

not completely amorphous but consists of a predominantly amorphous matrix containing minor crystalline constituents. Crystalline peaks associated with Fe_2O_3, MnO_2, MgO, and $CaMg(CO_3)_2$ can be identified. The occurrence of these crystalline phases may be related to the specific raw-material composition, ironmaking process, and cooling history of the industrial slag. Fe-, Mn-, and Mg-bearing components may remain in the slag during ironmaking, while locally slower cooling or incomplete vitrification may allow a small fraction of these components to crystallize. Therefore, the presence of these crystalline peaks does not indicate that the slag is predominantly crystalline, but rather reflects the coexistence of an amorphous glassy matrix with minor crystalline phases in the actual industrial slag. The amorphous glassy phase is considered to provide the major potential reactive fraction under alkaline activation. The main chemical compositions of the cement, fly ash, and desulfurized gypsum are listed in Table 4.

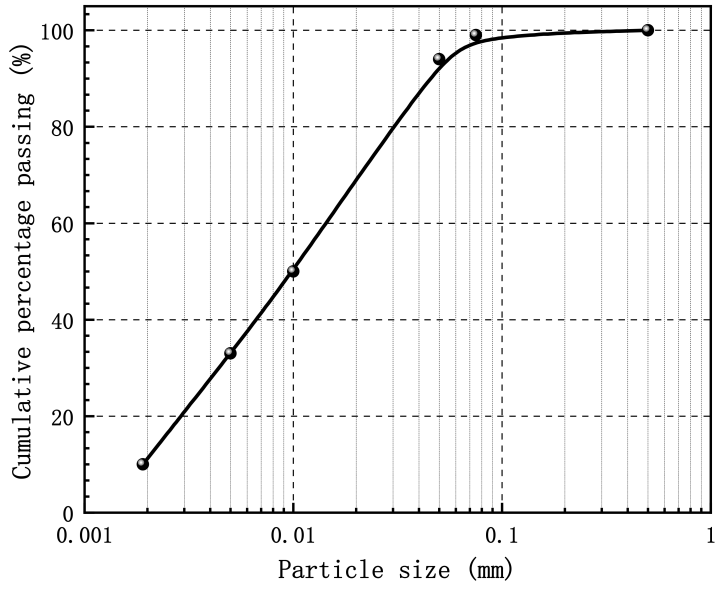


Figure 1. Particle-size distribution curve of the construction spoil.

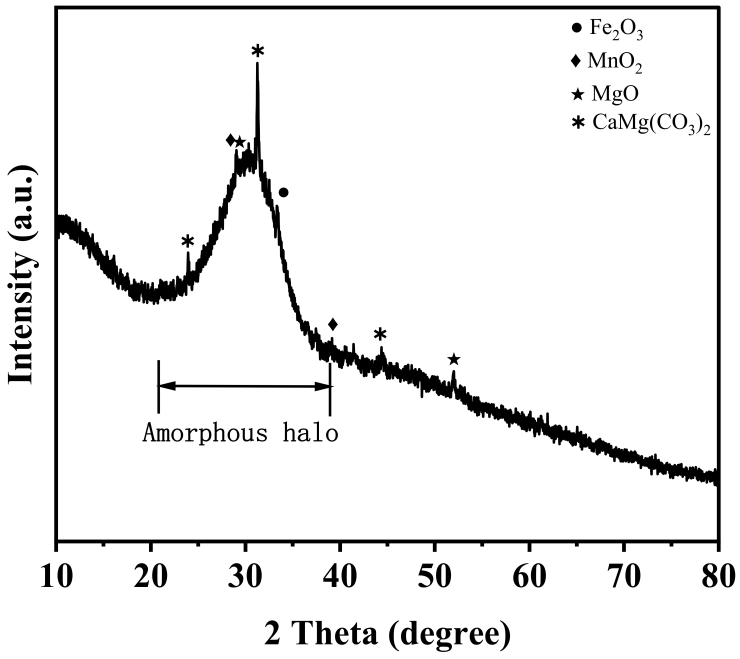


Figure 2. XRD pattern of the slag, showing the amorphous halo and minor crystalline phases.

Table 4. Main chemical compositions of the constituent materials of the solidifying agent.

Material	SiO_2	Al_2O_3	Fe_2O_3	CaO	SO_3	K_2O	MgO
Cement (%)	20.61	3.96	4.73	66.96	3.61	0.95	1.34
Fly ash (%)	34.50	16.70	1.50	35.30	1.24	--	5.01
Desulfurized gypsum (%)	--	--	--	35.9	43.1	--	--

The solidifying-agent content was determined using Equation (1):

$$\text{Solidifying-agent content } (\%) = \frac{m_s}{m_d} \quad (1)$$

where m_s and m_d are the masses of the solidifying agent and construction spoil, respectively.

Tap water was used in the tests. The water-to-solid ratio was defined as shown in Equation (2). The water-to-solid ratio used in all test series was 0.43. Unless otherwise stated, it was kept constant within each test series:

$$\text{Water-to-solid ratio} = \frac{m_\omega}{m_s + m_d} \quad (2)$$

where m_w is the mass of water.

To improve the reproducibility of the experimental program, the complete mass compositions of the 12 mixtures were normalized to 1000 g of dry excavated soil and are summarized in Table 5.

Table 5. Complete normalized mass proportions of the 12 mixtures.

Series	Mixture	Natural Soil/g	Solidifying Agent/g	Cement/g	Slag/g	Fly Ash/g	Gypsum/g	Activator Dosage/%	$Ca(OH)_2$/g	Na_2SO_4/g	Water/g	w/s	Slag:Fly Ash
Solidifying-agent content	S10	1000	100	20	30	35	15	3.8	2.375	1.425	473.0	0.43	30:35
	S12	1000	120	24	36	42	18	3.8	2.850	1.710	481.6	0.43	30:35
	S15	1000	150	30	45	52.5	22.5	3.8	3.563	2.138	494.5	0.43	30:35
	S20	1000	200	40	60	70	30	3.8	4.750	2.850	516.0	0.43	30:35
	S30	1000	300	60	90	105	45	3.8	7.125	4.275	559.0	0.43	30:35
Alkaline activator dosage	A1.8	1000	100	20	30	35	15	1.8	1.125	0.675	473.0	0.43	30:35
	A2.8	1000	100	20	30	35	15	2.8	1.750	1.050	473.0	0.43	30:35
	A3.8	1000	100	20	30	35	15	3.8	2.375	1.425	473.0	0.43	30:35
	A4.8	1000	100	20	30	35	15	4.8	3.000	1.800	473.0	0.43	30:35
Slag-to-fly ash ratio	F1–1	1000	100	20	32.5	32.5	15	4.8	3.000	1.800	473.0	0.43	1:1
	F1–1.5	1000	100	20	26	39	15	4.8	3.000	1.800	473.0	0.43	1:1.5
	F1–2	1000	100	20	21.67	43.33	15	4.8	3.000	1.800	473.0	0.43	1:2

All mixture masses were normalized to 1000 g of dry excavated soil. The solidifying-agent content was calculated relative to the dry mass of the excavated soil. The alkaline activator dosage was calculated relative to the total mass of the solidifying agent. The composite alkaline activator consisted of $Ca(OH)_2$ and Na_2SO_4 at a fixed mass ratio of 5:3. The water-to-solid ratio was fixed at 0.43, and the corresponding water mass for each mixture was calculated according to Equation (2). For the slag-to-fly ash series, the combined mass of slag and fly ash was kept constant while only their relative proportions were varied.

2.2. Experimental Methods

After collection, plant roots, gravel, and other impurities were first removed from the excavated soil, which was then air-dried, crushed, sieved, and sealed for storage. Before each test, the excavated soil, solidifying-agent constituents, and alkaline activator were weighed according to the designed mix proportions. The excavated soil was first dry-mixed with cement, slag, fly ash, and desulfurized gypsum. After uniform mixing, the pre-prepared alkaline activator solution and design water were added, and mixing

continued until a homogeneous slurry without visible agglomeration was obtained. Fresh mixtures were used for flow-spread and bleeding tests, while the remaining slurry was cast into the corresponding molds for mechanical and permeability tests.

After casting, the specimens were left undisturbed indoors for 24 h, demolded, and then cured at (20 ± 5) °C and relative humidity ≥ 95% for 3, 7, 14, and 28 d. At the specified curing age, the specimens were removed for the corresponding performance tests.

2.2.1. Determination of Flow Spread

The flowability test was conducted in accordance with the Technical Standard for Engineering Application of Premixed Flowable Solidified Soil (DBJ51/T 188-2022 [20]), as shown in Figure 3. Petroleum jelly was applied to the inner wall of an acrylic cylinder, which was then placed at the center of a transparent glass plate. The flowable solidified soil mixed with the solidifying agent was stirred uniformly, poured into a measuring cup, and then slowly poured into the acrylic cylinder. The outside of the cylinder was gently tapped with a straight-edged spatula to make the soil mixture more compact, and the top surface was leveled along the rim of the cylinder. The acrylic cylinder was then lifted vertically. After the solidified soil mixture collapsed and stood for 1 min, its spread diameter was measured using a steel ruler. The procedure was repeated three times, and the arithmetic mean of the three measurements was taken as the final flow-spread value.



Figure 3. Flow-spread test.

2.2.2. Determination of Bleeding Rate

The mixture was prepared in accordance with Test Method T 0589-2020 in the Test Methods of Cement and Concrete for Highway Engineering (JTG 3420-2020: Testing Methods of Cement and Concrete for Highway Engineering. China Communications Press: Beijing, China, 2020). The test procedure is shown in Figure 4. The total water content W and total mass G of the mixture were recorded. The inner wall of the measuring cylinder was wetted without visible free water, and its mass m_1 was measured to an accuracy of 1 g. The prepared mixture was then placed into two measuring cylinders, with the mixture surface approximately 10 mm below the rim. The total mass of the measuring cylinder and mortar specimen was recorded as m_2, also to an accuracy of 1 g. The cylinders were covered and left to stand. Within the first 30 min, bleeding water was extracted with a pipette every 15 min; thereafter, bleeding water was extracted every 30 min until no water could be extracted in three consecutive operations. The total mass of bleeding water, W_b, was then measured. During water extraction, one side of the measuring cylinder was slightly raised to allow the bleeding water to accumulate, and the water was drawn out with a pipette and transferred to a stoppered graduated cylinder. The cumulative bleeding amount was recorded each time. After each extraction, the measuring cylinder was gently returned to a horizontal position without disturbing the mixture. The bleeding rate was calculated using Equation (3). For the two test results, the difference between the maximum and minimum values should not exceed 15% of their average. The arithmetic mean of the

two measurements was taken as the test result and reported to the nearest 0.1%; otherwise, the test was repeated.

$$B_m = \frac{W_b}{(W/G)(m_2 - m_1)} \quad (3)$$

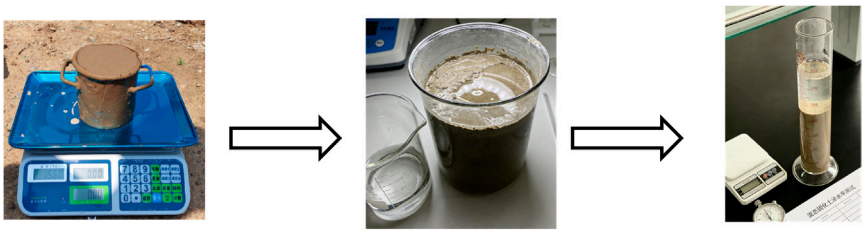


Figure 4. Bleeding-rate test.

2.2.3. Determination of Unconfined Compressive Strength

The test was conducted in accordance with ASTM D4832 [21]. Before testing, the engineering soil, constituent materials of the solidifying agent, composite alkaline activator, and mixing water were weighed according to the designed proportions. As shown in Figure 5, the engineering soil, cement, slag, fly ash, and desulfurized gypsum were first dry-mixed to uniformly disperse the solid constituents. The pre-prepared alkaline activator and mixing water were then added, and mixing continued until a homogeneous slurry without visible agglomerates was obtained. The mixture was cast into the corresponding molds. Specimens for UCS testing measured 70.7 × 70.7 × 70.7 mm, while ring cutters 61.8 mm in diameter and 40 mm in height were used for permeability specimens. After casting, the specimens were covered with plastic film to reduce early-age moisture loss.



Figure 5. Unconfined compressive strength test.

The specimens were demolded 48 h after casting and cured under standard conditions at (20 ± 2) °C and relative humidity ≥ 95% until 3, 7, 14, or 28 d. During the UCS test, the loading rate of the compression testing machine was set to 1 mm/min for controlled low-strength material specimens.

Three replicate specimens were prepared for each group, and the test result was reported as the arithmetic mean of three valid specimens. When complete replicate-level raw data were available, the standard deviation was also calculated. No data were subjectively excluded unless a specimen exhibited obvious damage, instrument malfunction, or a traceable operational anomaly.

2.2.4. Determination of Permeability Coefficient

The permeability test was conducted in accordance with the Specification for Mix Proportion Design of Cement Soil (JGJ/T 233-2011 [22]), as shown in Figure 6. Ring-cutter molds measuring 61.8 mm in diameter and 40 mm in height were used. Petroleum jelly was applied to the inner wall of each mold, the prepared CLSM was poured into the ring

cutter and compacted by vibration, and three replicate specimens were prepared for each group. The specimens were then cured in a constant-temperature and constant-humidity chamber at 20 °C and 95% relative humidity until the specified curing age. They were mounted in the permeability apparatus and tested according to the prescribed procedure. Readings were started when water seeped uniformly from the specimen surface. A test was terminated after the seepage rate became stable, and each specimen was measured at least six times.

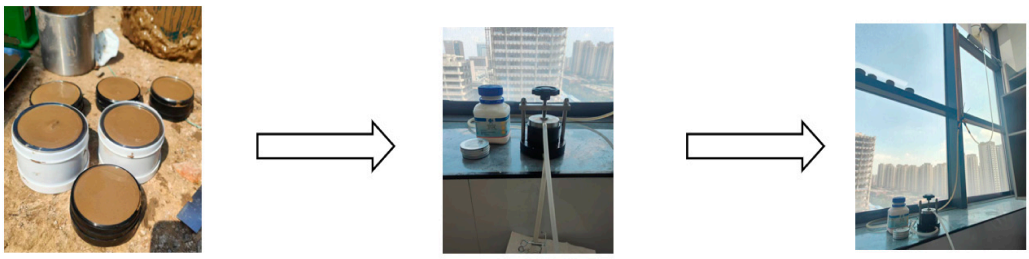


Figure 6. Permeability coefficient test.

3. Results and Discussion

3.1. Effect of Solidifying-Agent Content on the Properties of Flowable Solidified Soil

Solidifying-agent content has a substantial influence on the workability of flowable solidified soil, and either excessively high or excessively low contents may prevent the material from satisfying construction requirements. To isolate the effect of solidifying-agent content, a single-factor control method was adopted in this test series. Only the solidifying-agent content was varied, at levels of 10%, 12%, 15%, 20%, and 30%; the water-to-solid ratio was fixed at 0.43; the dosage of the composite alkaline activator consisting of anhydrous sodium sulfate and hydrated lime was fixed at 3.8%; and the solidifying-agent formulation comprised 35% fly ash, 20% cement, 30% slag, and 15% gypsum powder by mass (all percentages were calculated relative to the mass of the residual soil). The flow spread, bleeding rate, compressive strength, and permeability of flowable solidified soil at different solidifying-agent contents were investigated. The test results are presented in Table 6.

Table 6. Test results for the effects of solidifying-agent content on the workability and mechanical properties of flowable solidified soil.

Solidifying-Agent Content	Flow Spread/mm	Bleeding Rate/%	Compressive Strength/MPa				Permeability Coefficient/$\times 10^{-6}$ cm/s		
			3 d	7 d	14 d	28 d	7 d	14 d	28 d
10%	191	1.78	0.46	0.62	0.83	0.94	1.20	0.96	0.87
12%	208	2.10	0.54	0.75	0.89	1.08	0.67	0.63	0.58
15%	236	2.56	0.66	0.80	0.98	1.18	0.64	0.57	0.52
20%	226	2.21	0.83	1.09	1.34	1.73	0.48	0.44	0.39
30%	173	2.04	1.59	2.04	3.73	5.43	0.38	0.36	0.30

The effects of solidifying-agent content on the flow spread and bleeding rate of flowable solidified soil are shown in Figure 7. Both indicators first increased and then decreased as the solidifying-agent content increased. At a content of 10%, the flow spread was 191 mm and the corresponding bleeding rate was 1.78%. When the content increased to 12%, the flow spread increased to 208 mm and the bleeding rate to 2.10%. At 15%, the flow spread reached a peak of 236 mm and the bleeding rate also reached its maximum of 2.56%. When the content was further increased to 20%, the flow spread decreased to 226 mm and the bleeding rate to 2.21%. At 30%, the flow spread further decreased to 173 mm, with a bleeding rate of 2.04%. At the initial stage of increasing solidifying-agent content, the newly

added solidifying agent can reduce friction between soil particles through adsorption–dispersion and lubrication effects, improve slurry rheology, and thereby increase flow spread. Once the content exceeds a certain range, however, slurry viscosity increases substantially, the relative amount of free water becomes insufficient, and particle flocculation and aggregation may occur, resulting in reduced flowability. The change in bleeding rate is directly related to the water-binding effect of the solidifying agent and the development of internal microstructure. Previous studies indicate that C-S-H/C-A-S-H-type cementitious products may form in similar alkali-activated slag systems and partially fill interparticle pores. When the solidifying-agent content is within a reasonable range, the formation of C-S-H-type cementitious products can therefore be inferred. These products can effectively bind free water and fill internal pores, thereby suppressing bleeding. An excessively high solidifying-agent content, however, may disturb the original stability of the slurry, affect particle suspension and water distribution, and consequently cause fluctuations in bleeding rate [23,24].

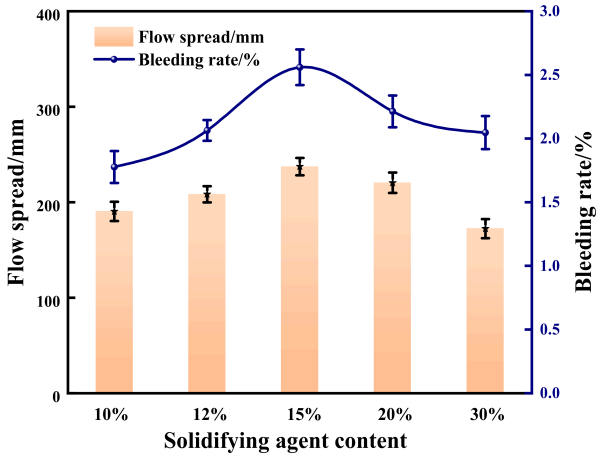


Figure 7. Variations in flow spread and bleeding rate of flowable solidified soil at different solidifying-agent contents.

The effect of solidifying-agent content on the time-dependent loss of flow spread is shown in Figure 8. Under all investigated contents, the flow spread continuously decreased with increasing standing time, exhibiting an overall monotonic decline. This indicates that, after mixing, hydration reactions continue within the slurry while the particle structure is progressively reconstructed, gradually increasing viscosity and causing irreversible loss of workability with time. From the mechanistic perspective, an appropriate amount of solidifying agent can optimize particle gradation and slurry rheology through fine-particle filling, adsorption–dispersion, and interfacial lubrication, thereby improving the initial flow spread. Early hydration products form a weakly cemented network that can partially restrain pore water and inhibit settlement and segregation, helping to slow the loss of flow spread. In contrast, when the solidifying-agent content is too low, the dispersion stability of the slurry is insufficient and flocculation becomes more pronounced; when the content is too high, the increased solid-phase volume fraction, relative shortage of free water, and accelerated water consumption by hydration intensify slurry thickening, causing both the initial flowability and time-dependent flow retention to decrease. Considering the initial flow spread together with its rate of loss, a solidifying-agent content of 15–20% provides a more reasonable balance between construction workability and slurry stability.

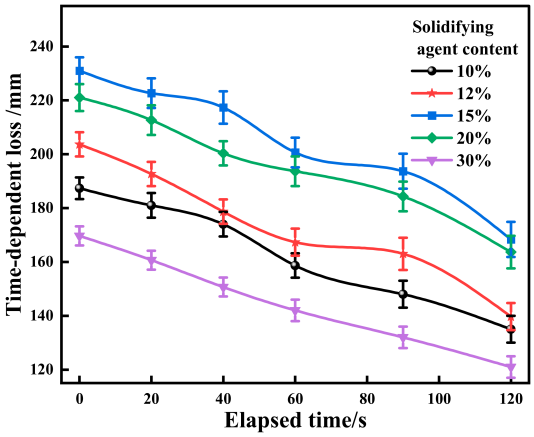


Figure 8. Time-dependent loss of flow spread of flowable solidified soil at different solidifying-agent contents.

The effect of solidifying-agent content on the compressive strength of flowable solidified soil is shown in Figure 9. The compressive strength at all curing ages increased continuously with increasing solidifying-agent content. At 10%, the 28-day compressive strength was 0.94 MPa; at 12%, 15%, 20%, and 30%, the corresponding 28-day strengths were 1.08, 1.18, 1.73, and 5.43 MPa, respectively. From a mechanics perspective, the continuous increase in strength with solidifying-agent content is associated with a higher proportion of cementitious phases and an improved soil microstructure. Based on previous studies, it can be inferred that hydration products such as C-S-H gel may form in similar alkali-activated slag systems and can effectively fill pores and increase compactness, thereby enhancing interparticle bonding stiffness and stress-transfer efficiency. This process improves the mechanical properties of the soil, reduces internal defects, inhibits the initiation and propagation of microcracks, enables more uniform load distribution, and ultimately increases the overall bearing capacity and compressive strength.

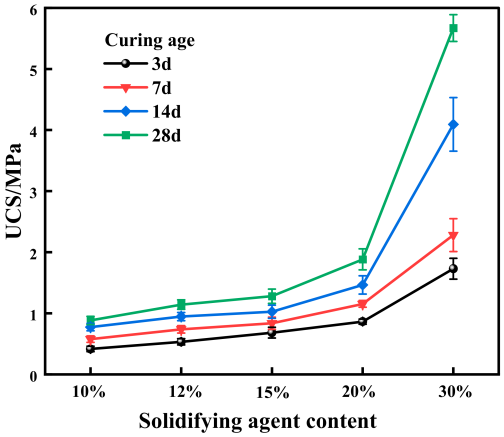


Figure 9. Variation in compressive strength of flowable solidified soil at different solidifying-agent contents.

The effect of solidifying-agent content on the permeability coefficient is shown in Figure 10. At the same curing age, the permeability coefficient generally decreased as the solidifying-agent content increased. Cementitious gels bond soil particles together, while hydration products fill internal pores and reduce the dimensions of seepage channels. The decrease in permeability coefficient was most pronounced when the solidifying-agent content increased from 10% to 12%. By contrast, the decrease became noticeably slower

as the content increased from 15% to 30%, indicating that the magnitude of permeability reduction gradually diminishes with increasing solidifying-agent content.

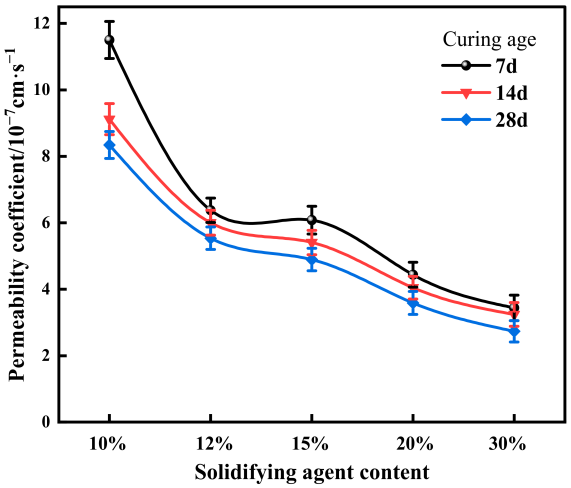


Figure 10. Variation in permeability coefficient of flowable solidified soil at different solidifying-agent contents.

The main reason is that, at relatively low solidifying-agent contents, hydration products preferentially fill large pores, substantially altering the internal pore structure and producing a large decrease in permeability. At higher contents, hydration products primarily refine smaller pores, so the rate of decrease in permeability slows [25]. With a continued increase in solidifying-agent content, the permeability coefficient tends to stabilize within a certain range. Thus, selecting an appropriate solidifying-agent content can effectively improve the internal soil structure, reduce permeability, and enhance the impermeability of flowable solidified soil.

To further evaluate the engineering applicability of the solidified soil, the 28-day permeability coefficients were compared with relevant engineering specifications. The measured permeability coefficients ranged from 3.03×10^{-7} to 8.72×10^{-7} cm/s. According to DB37/T 5350-2026 [26], no uniform permeability limit is specified for ordinary backfill applications; however, a permeability coefficient not exceeding 1.0×10^{-6} cm/s is required for recycled-material cutoff walls, while a more stringent value of 1.0×10^{-7} cm/s is recommended when the prevention of contaminant migration is required. The 28-day permeability coefficients obtained in this study were all lower than 1.0×10^{-6} cm/s, demonstrating the relatively low permeability of the developed material and indicating its potential for backfilling applications where seepage control is required. However, the values did not reach the more stringent 1.0×10^{-7} cm/s criterion for contaminant-barrier applications. For road-subgrade applications, permeability should be considered together with drainage, strength, and deformation requirements rather than as an independent acceptance criterion.

3.2. Effect of Alkaline Activator Dosage on the Properties of Flowable Solidified Soil

Alkaline activator dosage is one of the key factors affecting the hydration rate and degree of flowable solidified soil. By regulating the pH of the hydration system, the activator affects the dissolution rate of reactive components in solid-waste-based cementitious materials and thus the rate and extent of hydration reactions. Different activator dosages substantially affect workability, and either excessive or insufficient dosages may prevent the material from meeting construction requirements. To isolate the effect of activator dosage, a single-factor control method was adopted. Only the activator dosage was varied, at 1.8%, 2.8%, 3.8%, and 4.8%, while the water-to-solid ratio was fixed at 0.43. The solidifying-agent

formulation consisted of 35% fly ash, 20% cement, 30% slag, and 15% gypsum powder by mass, and the solidifying-agent content was fixed at 10% (all percentages were calculated relative to the mass of the residual soil). The flow spread, bleeding rate, and compressive strength at different alkaline activator dosages were investigated. The results are presented in Table 7.

Table 7. Test results for the effects of alkaline activator dosage on the workability and mechanical properties of flowable solidified soil.

Alkaline Activator	Dosage	Flow Spread/mm	Bleeding Rate/%	Compressive Strength/MPa				Permeability Coefficient/$\times 10^{-6}$ cm/s		
				3 d	7 d	14 d	28 d	7 d	14 d	28 d
Calcium hydroxide + anhydrous sodium sulfate	1.8%	214	2.4	0.32	0.45	0.58	0.68	5.80	4.20	3.17
	2.8%	205	1.7	0.42	0.58	0.72	0.83	4.90	3.74	2.18
	3.8%	198	0.8	0.45	0.61	0.75	0.88	3.00	2.14	1.63
	4.8%	193	0.3	0.51	0.65	0.79	0.92	0.67	0.61	0.54

The alkaline activator used in this study was a composite system consisting of calcium hydroxide and anhydrous sodium sulfate. The effect of activator dosage on workability is shown in Figure 11. As the dosage increased, the flow spread decreased gradually while the bleeding rate decreased markedly, indicating a negative correlation between the two indicators. At 1.8%, the flow spread was 214 mm and the bleeding rate was 2.4%; at 2.8%, the flow spread decreased to 205 mm and the bleeding rate to 1.7%; at 3.8%, the flow spread was 198 mm and the bleeding rate decreased sharply to 0.8%; and at 4.8%, the flow spread further decreased to 193 mm while the bleeding rate was only 0.3%. Within the investigated range, the total reduction in flow spread was approximately 9.8%, whereas the bleeding rate decreased by 87.5% [27], demonstrating a much stronger effect of the activator on bleeding control. Although increasing activator dosage reduced flowability to some extent, it enhanced water retention. Microscopically, the rise in pH with activator dosage accelerates dissolution of reactive components and hydration reactions in the solid-waste-based cementitious material, increasing the amount of hydration products and progressively forming a stable spatial skeleton. This structure effectively restrains free-water migration and particle settlement, thereby reducing bleeding. Densification also increases internal frictional resistance and causes a slight decrease in flow spread. At relatively high dosages, the material can therefore maintain good flowability while effectively suppressing bleeding, resulting in favorable workability.

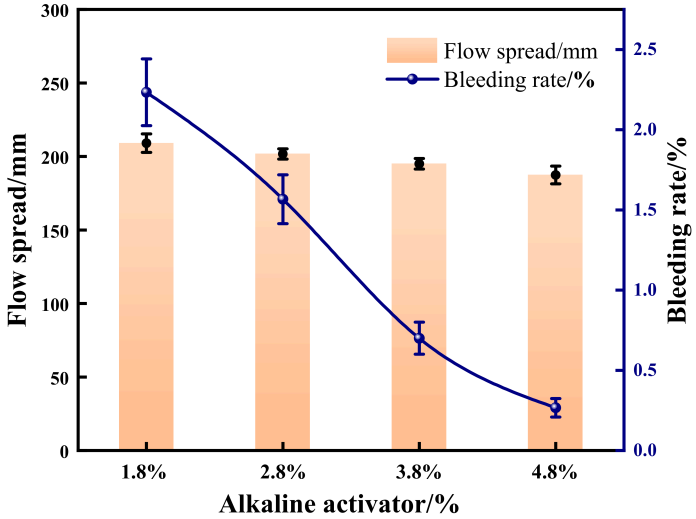


Figure 11. Variations in flow spread and bleeding rate of flowable solidified soil at different alkaline activator dosages.

As shown in Figure 12, the compressive strength of flowable solidified soil increased continuously with curing age at all alkaline activator dosages. At a dosage of 1.8%, the 28-day compressive strength was approximately 0.68 MPa; it increased to 0.83 MPa at 2.8%, 0.88 MPa at 3.8%, and 0.92 MPa at 4.8%. Overall, compressive strength increased distinctly with activator dosage, and the strength gains at different curing ages were relatively stable; comparatively, the strength-enhancement effect was particularly evident at higher dosages [28,29].

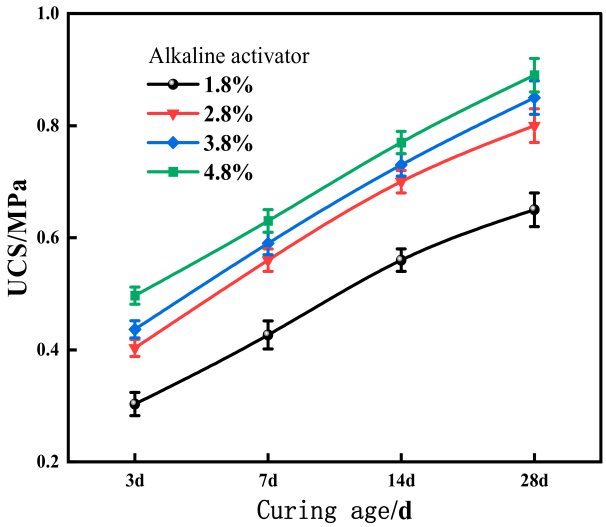


Figure 12. Variation in compressive strength of flowable solidified soil at different alkaline activator dosages.

Notably, under relatively high alkaline activator dosages, the strength gain from 14 to 28 d was smaller than that at earlier ages. This indicates that increasing activator dosage does not maintain the same proportional increase in later-age strength. One possible explanation is that higher alkalinity promotes the early dissolution and reaction of active components, so that part of the potentially reactive material is already consumed more extensively at early ages. As curing proceeds, fewer active components remain available for further reaction, and the later-age strength-development rate therefore decreases. In addition, rapid accumulation of early reaction products on particle surfaces may restrict subsequent ion transport and continuing reactions. Because hydration heat and quantitative reaction-kinetics tests were not conducted in this study, this interpretation is proposed primarily on the basis of the macroscopic strength-development trend together with the relevant literature.

From a materials-mechanics perspective, increasing alkaline activator dosage increases the proportion of cementitious phases in the system and accelerates hydration. More hydration products, including C-S-H gel, fill internal pores, substantially increase compactness, and enhance interparticle bonding stiffness and stress-transfer efficiency. This process improves the material microstructure, reduces internal defects, inhibits microcrack initiation and propagation, and ultimately increases the overall bearing capacity and compressive strength of the flowable solidified soil. Consequently, the mechanical properties improve progressively with increasing alkaline activator dosage.

As shown in Figure 13, at the same curing age the permeability coefficient decreased markedly with increasing activator dosage, and this trend was consistent at 7, 14, and 28 d, indicating that alkaline activator dosage is a key factor controlling the impermeability of this recycled material. When the activator dosage increased from 1.8% to 2.8%, the permeability coefficient decreased from 5.80×10^{-6} cm/s to 4.90×10^{-6} cm/s. It then

decreased rapidly to 3.00 × 10^{-6} cm/s at 3.8% and further to 0.67 × 10^{-6} cm/s at 4.8%, demonstrating a substantial improvement in impermeability in the high-dosage range.

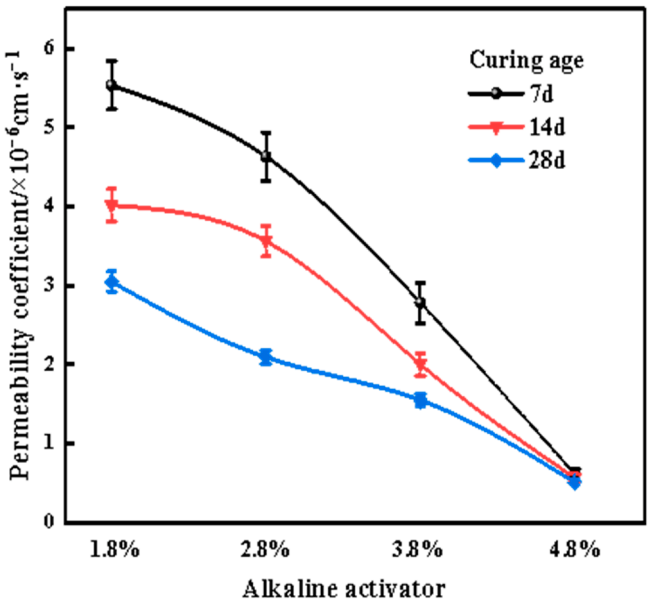


Figure 13. Variation in permeability coefficient of flowable solidified soil at different alkaline activator dosages.

At the microscopic level, when the activator dosage is low, the number of alkaline ions available for reaction is insufficient and only the initial dissolution of reactive silica-alumina components in the construction spoil can be promoted. The resulting gel products preferentially fill large pores, partly improving the original pore structure and reducing permeability. At a moderate dosage, the substantially higher alkalinity promotes polymerization of more reactive components and the formation of a continuous, dense aluminosilicate gel network. This network effectively bonds soil particles and greatly reduces pore connectivity, causing a further decrease in permeability. At a relatively high dosage, reaction products can sufficiently fill large pores while refining smaller pores, so the internal structure becomes progressively denser and more stable and seepage pathways are substantially reduced. The permeability coefficient continues to decrease, although its rate of decrease is slower than in the moderate-dosage range. With increasing curing age, the activation reaction continues and the gel structure develops further, so permeability decreases for all dosages; the long-term impermeability advantage is more pronounced for high-dosage specimens. Appropriately increasing activator dosage can therefore effectively improve pore structure and impermeability, but the benefit exhibits diminishing returns. In engineering applications, the optimum dosage should be determined by considering both material performance and economy.

3.3. Effects of Slag-to-Fly Ash Ratio on the Properties of Flowable Solidified Soil

To reduce cement consumption and increase the utilization of solid wastes, large quantities of alkali-activated slag and fly ash were used to prepare flowable solidified soil, and the effects of their proportions on the physical and microstructural properties were investigated. A controlled-variable method was used to examine the influence of the slag-to-fly ash proportion. The solidifying-agent content was fixed at 10%, with a formulation of cement:gypsum powder:(fly ash + slag) = 4:3:13 and an activator dosage of 4.8% (all percentages were calculated relative to the mass of the residual soil), and the water-to-solid ratio was 0.43. The flow spread, bleeding rate, and compressive strength of

flowable solidified soil at different slag and fly ash contents were investigated. The test results are presented in Table 8.

Table 8. Test results for the effects of slag-to-fly ash ratio on the workability and mechanical properties of flowable solidified soil.

Slag-To-Fly Ash Ratio	Flow Spread/mm	Bleeding Rate/%	Compressive Strength/MPa				Permeability Coefficient/$\times 10^{-6}$ cm/s		
			3 d	7 d	14 d	28 d	7 d	14 d	28 d
1:1	185	1.22	0.54	0.80	0.98	1.37	3.40	2.60	2.05
1:1.5	205	1.68	0.46	0.75	0.83	1.08	2.90	2.10	1.65
1:2	226	1.96	0.37	0.68	0.79	0.93	2.60	1.95	1.50

The effects of different slag-to-fly ash proportions on the flow spread and bleeding rate are shown in Figure 14. Both the flow spread and bleeding rate increased continuously as the proportion changed. At a slag-to-fly ash ratio of 1:1, the initial flow spread was 185 mm and the bleeding rate was 1.22%; at 1:1.5, they increased to 205 mm and 1.68%, respectively; and at 1:2, they reached 226 mm and 1.96%. This behavior arises because variations in fly ash and slag contents jointly regulate workability by changing chemical reactivity, particle gradation, and rheology. When the fly ash content decreases, its hydration reaction weakens, fewer cementitious hydration products are generated, and mixture bonding decreases; simultaneously, the physical filling effect of fly ash as fine particles is weakened and system porosity increases. Together, these effects reduce slurry viscosity and relatively increase free water, producing higher flowability and making water more likely to separate and migrate upward, thereby increasing the bleeding rate. Slag particles have irregular morphologies, and increasing slag content enhances mechanical interlocking and friction between particles, hindering slurry flow. Slag surfaces also readily adsorb water and admixtures, forming an adhesive layer that further increases viscosity. Increasing slag content therefore reduces flowability and bleeding. Variations in the contents of the two materials jointly affect the flowability and bleeding characteristics of flowable solidified soil through their different effects on the chemical and physical structures of the slurry.

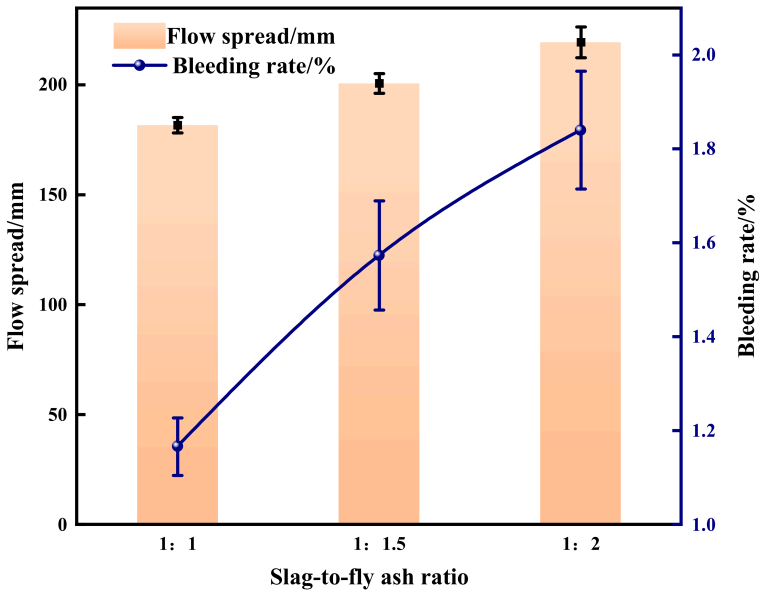


Figure 14. Variations in flow spread and bleeding rate of flowable solidified soil at different slag-to-fly ash ratios.

The effect of different slag-to-fly ash proportions on compressive strength is shown in Figure 15. At a slag-to-fly ash ratio of 1:1, the 28-day compressive strength was 1.37 MPa; at 1:1.5, it was 1.08 MPa; and at 1:2, it was 0.93 MPa. The effect of the slag-to-fly ash mass ratio on the unconfined compressive strength of the flowable solidified soil is shown in Figure 15. When the slag-to-fly ash mass ratio was 1:1, the 28-day unconfined compressive strength of the specimen was 1.37 MPa. When the ratio was adjusted to 1:1.5 and 1:2, the corresponding 28-day unconfined compressive strengths decreased to 1.08 MPa and 0.93 MPa, respectively. Overall, with an increase in the relative proportion of fly ash and a corresponding decrease in the relative proportion of slag, the compressive strength of the specimens decreased at all curing ages. In particular, when the slag-to-fly ash mass ratio changed from 1:1 to 1:2, the 28-day strength decreased by approximately 32.1%.

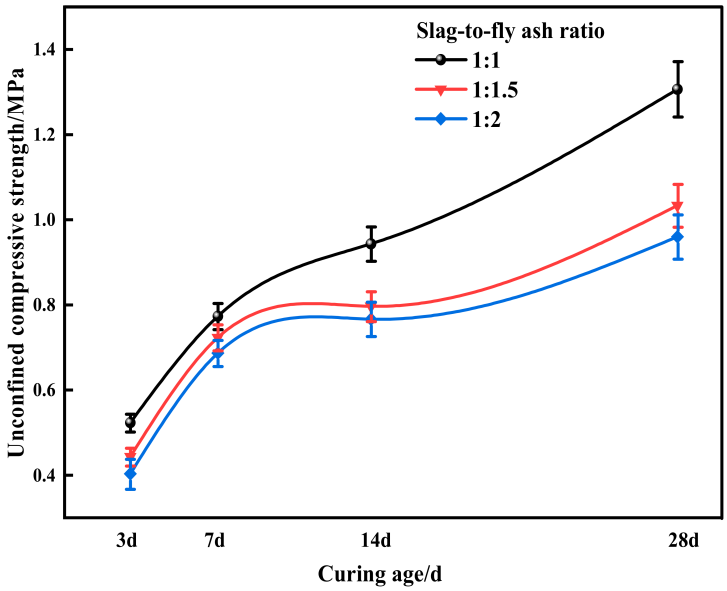


Figure 15. Variation in compressive strength of flowable solidified soil at different slag-to-fly ash ratios.

These results indicate that variations in the slag-to-fly ash ratio exert different effects on the workability and mechanical properties of the material. Previous studies have shown that fly ash particles generally possess a relatively spherical morphology, and their ball-bearing effect can reduce interparticle friction while improving particle packing and slurry flowability. Therefore, as the proportion of fly ash increases, its physical contribution does not disappear but is mainly reflected in the improvement in flow spread. In contrast, slag generally exhibits higher early-age reactivity under alkaline activation and can participate more rapidly in the cementitious reaction, thereby promoting the formation of a bonded structure. Fly ash typically exhibits a relatively lower early-age reaction rate. Consequently, when the relative slag content decreases and the proportion of fly ash increases, the amount of highly reactive components available at early ages and the rate of formation of the cementitious structure may both decrease, which is unfavorable for strength development [30,31].

Therefore, at a slag-to-fly ash mass ratio of 1:2, it would be inappropriate to conclude that the physical filling or ball-bearing effect of fly ash is completely offset. On the contrary, the increased fly ash content continues to provide beneficial physical effects on the workability of the slurry. However, in terms of compressive strength, these physical benefits are insufficient to compensate for the reduced cementitious reactivity associated with the lower slag content, ultimately resulting in a trade-off characterized by improved flowability but reduced compressive strength. This trend is generally consistent with findings reported

for alkali-activated slag–fly ash systems, in which increasing the proportion of fly ash commonly improves slurry flowability, whereas a high fly ash replacement level may limit early- and medium-term strength development because of slower reaction kinetics and a reduced proportion of highly reactive Ca-rich components [25]. It should be noted that early-age calorimetry and hardened-state microstructural characterization were not conducted in the present study. Therefore, the above interpretation is based primarily on the macroscopic experimental results obtained in this study and reaction mechanisms reported in the literature. The detailed reaction process should be further verified by techniques such as isothermal calorimetry, XRD, and SEM.

It is also worth noting that when the slag-to-fly ash mass ratio changed from 1:1 to 1:2, the flow spread increased from 185 mm to 226 mm, whereas the 28-day unconfined compressive strength decreased from 1.37 MPa to 0.93 MPa. This further demonstrates that increasing the proportion of fly ash can improve construction workability at the expense of a certain degree of mechanical performance. Therefore, the slag-to-fly ash ratio should be selected by comprehensively considering both workability requirements and strength requirements.

As shown in Figure 16, at the same curing age the permeability coefficient generally decreased as the fly ash proportion in the slag-to-fly ash ratio increased. At 28 d, the ratios of 1:1, 1:1.5, and 1:2 corresponded to permeability coefficients of 2.05×10^{-6}, 1.65×10^{-6}, and 1.50×10^{-6} cm/s, respectively, indicating that increasing the fly ash content can improve impermeability. For all ratios, permeability decreased markedly with increasing curing age; the reduction from 7 to 14 d was most pronounced, whereas the decrease from 14 to 28 d gradually slowed. This indicates that the pore structure evolves rapidly at early ages and progressively stabilizes during middle and later curing. The main reason is that both slag and fly ash possess latent reactivity. Fly ash particles are finer and have a larger specific surface area; in an alkaline environment they can undergo secondary hydration with $Ca(OH)_2$ in the hydration products, generating additional C-S-H gel that continuously fills existing soil pores, promotes the transformation of large pores into medium and small pores, and effectively reduces the connectivity of seepage pathways. Increasing fly ash content further increases structural compactness. The decrease in permeability was relatively pronounced when the ratio changed from 1:1 to 1:1.5, but became smaller when it changed from 1:1.5 to 1:2. This indicates that, in the high-fly-ash-content range, pore filling and structural densification progressively stabilize and the rate of permeability improvement slows. An appropriate increase in fly ash content can therefore reduce permeability, optimize internal pore structure, and improve the overall impermeability of flowable solidified soil [25].

When the slag-to-fly ash mass ratio was adjusted from 1:1 to 1:2, the flow spread increased from 185 mm to 226 mm, an increase of approximately 22.2%; the 28-day UCS decreased from 1.37 MPa to 0.93 MPa, a reduction of approximately 32.1%. Meanwhile, the 28-day permeability coefficient decreased from 2.05×10^{-6} cm/s to 1.50×10^{-6} cm/s.

These results indicate that the physical effects associated with increasing the fly ash proportion are not completely offset by the adverse influence of its lower reactivity; rather, the outcome clearly depends on the performance indicator considered. In terms of workability, a higher fly ash proportion is beneficial to slurry flowability. In terms of mechanical performance, reducing the slag proportion decreases the amount of highly reactive cementitious components and therefore lowers the 28-day strength. In terms of permeability, however, fine-particle filling and possible later-age pozzolanic reactions may still help reduce the connectivity of seepage pathways. Therefore, the 1:2 ratio should not simply be defined as the best or worst mixture; instead, it should be selected comprehensively according to the required flowability, strength, and impermeability for the specific engineering application.

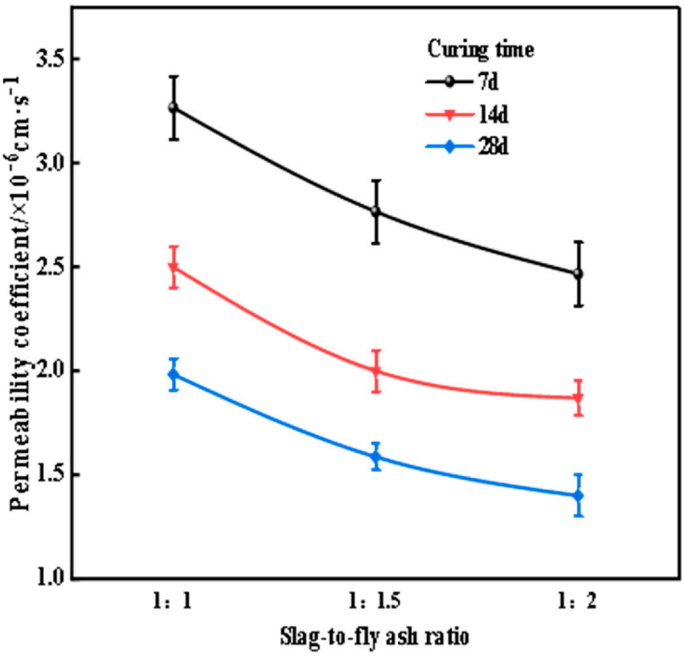


Figure 16. Variation in permeability coefficient of flowable solidified soil at different slag-to-fly ash ratios.

4. Performance Trade-Offs and Engineering Applicability Under Different Mix-Proportion Parameters

A single-factor control method was used to separately evaluate the effects of solidifying-agent content, composite alkaline activator dosage, and slag-to-fly ash ratio on the properties of flowable solidified soil. Therefore, the present test results primarily reflect the sensitivity of each parameter under the specified baseline conditions and cannot yet be used to quantitatively evaluate interactions among the parameters.

The influence of solidifying-agent content on solidified-soil performance exhibits an evident nonlinear pattern. At relatively low contents, physical filling and dispersion by fine particles dominate, effectively improving slurry rheology and increasing flowability. Once the content exceeds 20%, the solid-phase volume fraction increases, the relative amount of free water becomes insufficient, and hydration products form rapidly, causing slurry viscosity to increase and flowability to decrease. In contrast, compressive strength and impermeability continue to improve as the solidifying-agent content increases. In particular, at 30% content, the 28-day compressive strength reaches 5.43 MPa, indicating the formation of a denser network of hydration products. The optimal ranges for flowability, strength, and impermeability are therefore clearly misaligned: the range giving the best flowability does not coincide with the range in which strength and impermeability continue to improve. Mix-proportion design must consequently balance construction workability with the long-term durability of the solidified soil.

The addition of alkaline activator substantially expands the adjustable performance range of the solidified system. When its dosage increases from 1.8% to 4.8%, system pH rises, accelerating dissolution of reactive components and formation of hydration products. Although this process causes a slight decrease in flowability, the bleeding rate decreases markedly from 2.4% to 0.3%, indicating that alkaline activation significantly improves the system's ability to restrain free water. Compressive strength increases continuously with alkaline activator dosage, although the rate of increase gradually narrows in the high-dosage range. The reduction in permeability coefficient is most pronounced at high dosage, further confirming that alkaline activation promotes the formation of a dense

microstructure. Alkaline activator dosage is therefore not only a parameter controlling strength but also a key indicator for optimizing workability and impermeability.

The slag-to-fly ash ratio reflects the synergistic effect of chemical reactivity and physical filling. Increasing the fly ash proportion can improve slurry rheology and flowability through the ball-bearing effect of its spherical particles, but may reduce the strength and impermeability of the solidified soil. Increasing the slag proportion, by contrast, promotes a denser internal structure through fine-particle filling and stronger secondary hydration activity, thereby increasing strength and reducing permeability, but it may also inhibit slurry flowability. Changes in the relative proportions of the two materials thus directly reflect the trade-off between workability and mechanical performance.

Future research may use Taguchi designs, orthogonal experiments, or response surface methodology to establish multifactor test schemes and quantitatively analyze interactions among solidifying-agent content, alkaline activator dosage, water-to-solid ratio, and slag-to-fly ash ratio. In addition, the three parameter groups should be co-optimized in accordance with actual engineering requirements to identify an optimal balance.

5. Conclusions

(1) Within the investigated range, solidifying-agent content affected the workability and strength of flowable solidified soil in different ways. As the content increased from 10% to 30%, the flow spread first increased from 191 mm to 236 mm and then decreased to 173 mm, whereas the 28-day unconfined compressive strength increased continuously from 0.94 MPa to 5.43 MPa. This indicates that a higher solidifying-agent content is beneficial to strength development but does not necessarily favor the retention of slurry flowability.

(2) With increasing solidifying-agent content and curing age, the permeability coefficient of flowable solidified soil generally decreased. When the solidifying-agent content increased from 10% to 30%, the 28-day permeability coefficient decreased from 8.72×10^{-7} cm/s to 3.03×10^{-7} cm/s. However, the magnitude of the reduction progressively decreased as the content increased further, indicating diminishing gains in impermeability from simply increasing the amount of solidifying agent.

(3) When the alkaline activator dosage increased from 1.8% to 4.8%, the flow spread decreased from 214 mm to 193 mm and the bleeding rate decreased from 2.4% to 0.3%; the 28-day unconfined compressive strength increased to 0.92 MPa, while the 28-day permeability coefficient decreased to 0.54×10^{-6} cm/s. The results indicate that increasing the activator dosage helps suppress bleeding and improves strength and impermeability, but causes a certain loss of flowability.

(4) When the slag-to-fly ash mass ratio was adjusted from 1:1 to 1:2, the flow spread increased from 185 mm to 226 mm, the 28-day UCS decreased from 1.37 MPa to 0.93 MPa, and the 28-day permeability coefficient decreased from 2.05×10^{-6} cm/s to 1.50×10^{-6} cm/s. Thus, adjusting the slag-to-fly ash ratio produces clear trade-offs among workability, mechanical performance, and permeability, and the mix proportion should be selected according to the functional requirements of the specific project.

(5) The single-factor tests established the basic response relationships between solidifying-agent content, alkaline activator dosage, and slag-to-fly ash ratio and the flowability, bleeding, strength, and permeability of the material, but they cannot quantify interactions among different factors. Future work may combine multifactor experimental design with SEM, MIP, quantitative XRD, and hydration-heat analysis to further optimize the mix proportion and investigate the underlying mechanisms.

Author Contributions: Conceptualization, H.M., G.S. and D.Z.; Methodology, G.S.; Validation, H.M. and J.H.; Investigation, D.H., W.L. and D.Z.; Resources, G.S. and D.H.; Data curation, J.H.; Writing—original draft, G.S.; Writing—review & editing, W.L.; Visualization, W.L. All authors have read and agreed to the published version of the manuscript.

Funding: This research was supported by the Science and Technology Project of Jinan Senyuan Holding Co., Ltd., "Research on Key Technologies for Multi-Source Solid Waste Backfilling and Prefabricated Foundations under a Green and Low-Carbon Orientation" (No. 520669250002).

Data Availability Statement: The raw data supporting the conclusions of this article will be made available by the authors on request.

Conflicts of Interest: Authors Haitao Ma, Dexiang Hou and Daoyuan Zhao were employed by the company Jinan Luyuan Electric Group Co., Ltd. The remaining authors declare that the research was conducted in the absence of any commercial or financial relationships that could be construed as a potential conflict of interest.

References

1. Lai, C.H.; Bai, Y.; Zhu, J.R.; Shi, J.L.; Duan, M.; Li, M.J. Experimental study on the optimum mix proportion and physical-mechanical properties of cement-solidified soil. *J. Xi'an Univ. Archit. Technol. (Nat. Sci. Ed.)* **2026**, *58*, 26–34. (In Chinese) [CrossRef]
2. Dai, H.J.; Wu, G.X.; Li, H.F.; Zhou, X.; Zhang, R. Study on the workability of flowable soil solidified by cement in combination with industrial solid wastes. *Bull. Chin. Ceram. Soc.* **2025**, *44*, 4492–4502. (In Chinese)
3. Li, Y.X.; Wang, Q.; Zhang, Q.C.; Zhou, L.A.; Mu, J. Effects of inorganic solidifying agents on the structure and properties of flowable solidified soil. *Mater. Rep.* **2023**, *37*, 156–162. (In Chinese)
4. Zhou, Y.X.; Wang, J.Z. Principle and engineering application prospects of premixed solidified soil. *New Build. Mater.* **2019**, *46*, 117–120. (In Chinese)
5. Su, Y.; Yan, N.; Bai, X.Y.; Fu, L.; Zhang, Q.; Liang, B.; Wang, B.; Wang, L.; Zhang, Y.; Zhang, A. Research progress and application of engineering properties of premixed flowable solidified soil. *Mater. Rep.* **2024**, *38*, 66–72. (In Chinese)
6. Zhu, W.; Zhao, D.; Fan, X.H.; Wu, S.; Wu, Y. Application of excavated soil improved as flowable backfill. *J. Hohai Univ. (Nat. Sci.)* **2021**, *49*, 134–139. (In Chinese)
7. Lyu, J.; Yang, J.; Liu, C.; Guan, X.; Moon, J.; Feng, S.; Zhang, J.; Ge, Z.; Zhang, H. Effect of carbonation curing time during early age on mechanical and microstructural properties of cement-based materials incorporating superabsorbent polymers. *J. Build. Eng.* **2026**, *120*, 115464. [CrossRef]
8. Sun, D.; Han, J.; Zhao, W.; Han, Y.; Peng, G. Sustainable utilization of shield waste muck for synchronous grouting: Mixture ratio optimization and assessment of environmental and economic performance. *Tunn. Undergr. Space Technol.* **2026**, *168*, 107190. [CrossRef]
9. Wang, H.L.; Zou, F.; Gao, S.L.; Sun, C.; Huang, J. Preparation and engineering application of flowable solidified soil using alkali-activated slag. *New Build. Mater.* **2025**, *52*, 140–145. (In Chinese)
10. Xie, T.L.; Li, C.H.; Tang, J.; Ding, J.W.; Wang, S.J. Properties of flowable solidified soil prepared from pipe-jacking spoil modified with various admixtures. *Geotech. Investig. Surv.* **2025**, *53*, 1–8+33. (In Chinese)
11. Chi, L.; Wang, X.L.; Liao, B.; Liu, T.; Wang, X. Study on multi-component composite solidifying agents for flowable solidified soil in the Shanghai area. *J. Build. Mater.* **2026**, *29*, 632–638. (In Chinese)
12. Hao, W.R.; Tang, L.; Wu, R.D.; Li, G.; He, W.; Yu, H. Performance optimization and application of flowable solidified soil prepared with all-solid-waste low-carbon cementitious materials. *Mater. Rep.* **2025**, *39*, 499–504. (In Chinese)
13. Feng, S.; Xiao, H.; Chen, L. Influence of nanomaterials on mechanical performance and microstructure of cement paste. *Constr. Build. Mater.* **2026**, *509*, 145146. [CrossRef]
14. Jalal, F.E.; Jamhiri, B.; Naseem, A.; Hussain, M.; Iqbal, M.; Onyelowe, K. Isolated Effect and Sensitivity of Agricultural and Industrial Waste Ca-Based Stabilizer Materials (CSMs) in Evaluating Swell Shrink Nature of Palygorskite-Rich Clays. *Adv. Civ. Eng.* **2021**, *2021*, 7752007. [CrossRef]
15. Gautam, S.; Hoyos, L.R.; He, S.; Prabakar, S.; Yu, X. Chemical Treatment of a Highly Expansive Clay Using a Liquid Ionic Soil Stabilizer. *Geotech. Geol. Eng.* **2020**, *38*, 4981–4993. [CrossRef]
16. Huang, J.; Makhatova, A.; Kogbara, R.; Masad, E.; Sukhishvili, S.; Little, D. Mechanical Properties of Palygorskite Clay Stabilized with Polyelectrolytes. *Transp. Geotech.* **2023**, *43*, 101124. [CrossRef]
17. Sharma, A.K.; Sivapullaiah, P.V. Ground Granulated Blast Furnace Slag Amended Fly Ash as an Expansive Soil Stabilizer. *Soils Found.* **2016**, *56*, 205–212. [CrossRef]

18. Parhizkar, A.; Nazarpour, A.; Khayat, N. Investigation of Geotechnical and Microstructure Characteristics of Gypsum Soil Using Ground Granulated Blast-Furnace Slag (GGBS), Fly Ash, and Lime. *Constr. Build. Mater.* **2024**, *418*, 135358. [CrossRef]
19. *GB/T 50123-2019*; Standard for Geotechnical Testing Method. China Planning Press: Beijing, China, 2019.
20. *DBJ51/T 188-2022*; Technical Standard for Engineering Application by Using Premixed Fluidized Stabilized Soil. Southwest Jiaotong University Press: Chengdu, China, 2022.
21. *ASTM D4832*; Standard Test Method for Preparation and Testing of Controlled Low Strength Material (CLSM) Cylindrical Test Specimens. ASTM International: West Conshohocken, PA, USA, 2023.
22. *JGJ/T 233-2011*; Specification for Mix Proportion Design of Cement Soil. China Architecture & Building Press: Beijing, China, 2011.
23. Cui, X.; Meng, H.; Liu, Z.; Sun, H.; Zhang, X.; Jin, Q.; Wang, L. Development, Performance, and Mechanism of Fluidized Solidified Soil Treated with Multi-Source Industrial Solid Waste Cementitious Materials. *Buildings* **2025**, *15*, 864. [CrossRef]
24. Chen, S.; Feng, C.; Fu, T.; Yu, D.; Zhang, H.; Zhang, F.; Wang, Y.; Huang, X.; Wang, Y. Performance and Characterization of Fluidized Solidified Soil Prepared by Synergistic Cement and Phosphogypsum with Slag Powder-Fly Ash. *J. Wuhan Univ. Technol.-Mater. Sci. Ed.* **2025**, *40*, 1320–1329. [CrossRef]
25. Sun, T.; Liu, Y.; Wang, Z.Y.; Ouyang, G.S.; Qin, T.X. Effect mechanism of phosphogypsum on the mechanical and impermeability properties of soft clay solidified by a slag-cement cementitious system. *Bull. Chin. Ceram. Soc.* **2025**, *44*, 4480–4491. (In Chinese)
26. *DB37/T 5350-2026*; Technical Standard for Application in Engineering of Building Solid Waste Recycling Materials. China Architecture & Building Press: Beijing, China, 2026.
27. Xing, Z.R.; Cui, Y.L.; Weng, M.X. Engineering properties of flowable solidified soil prepared from alkali-activated cementitious waste slurry. *J. Wuhan Univ. Technol.* **2025**, *47*, 9–15. (In Chinese)
28. Li, H.Z.; Wu, S.X.; Chen, C.; Yin, S.; Wang, L.; Zhu, K.; Feng, Z. Mechanical and durability properties of flowable solidified soil based on waste slurry from pile foundation construction. *China Foreign Highw.* **2025**, *45*, 35–45. (In Chinese)
29. Liu, L.; Yao, Y.; Zhang, L.L.; Liang, T.; Hu, Y. Effect of alkali content on the properties of silty clay solidified by alkali-activated cementitious materials. *Mater. Rep.* **2026**, *40*, 135–145. (In Chinese)
30. Wang, Y.; Gu, X.-W.; Xu, X.-C.; Wang, Q. Hydration Characteristics of Slag-Fly Ash Cementitious System Activated by Lime-Sodium Sulfate Composite. *J. Northeast. Univ. (Nat. Sci.)* **2025**, *46*, 87–96. (In Chinese)
31. Lyu, C.H. Preparation and mechanical properties of cement-slag-fly ash flowable solidified soil. *Eng. Technol. Res.* **2025**, *10*, 115–117. (In Chinese)

Disclaimer/Publisher's Note: The statements, opinions and data contained in all publications are solely those of the individual author(s) and contributor(s) and not of MDPI and/or the editor(s). MDPI and/or the editor(s) disclaim responsibility for any injury to people or property resulting from any ideas, methods, instructions or products referred to in the content.